Chapter 12

Flow Control Using Flapping Wings for an Efficient Low-Speed Micro-Air Vehicle

Kevin D. Jones and Max F. Platzer

Abstract A review is given of the research studies which led to the development of a flapping-wing propelled micro air vehicle which uses two oscillating wings in a biplane arrangement for propulsion and a fixed wing for lift generation. Computational and experimental studies are described which were conducted to obtain quantitative information about the thrust and propulsive efficiency offered by this choice. They included inviscid incompressible panel code as well as viscous Navier-Stokes computations, flow visualizations and flow measurements in water and wind tunnels as well as direct thrust measurements. It is shown that the placement of the fixed wing upstream but closely coupled to the two oscillating wings delays flow separation and therefore offers special advantages for flight operations at the low Reynolds numbers encountered by micro air vehicles.

12.1 Introduction

The mastery of flight exhibited by birds and insects has fascinated man for many centuries and has induced his longing for wings of his own. However, various attempts throughout history to emulate bird flight, as documented, for example, by Dalton [6] remained unsuccessful. The German flight pioneer Otto Lilienthal [15] summarized the results of his studies of storks and other birds in a book titled "Bird flight as the Basis for Human Flight," published in 1889. He thus contributed greatly to the understanding of flapping-wing aerodynamics. In particular, he correctly identified the drag reduction (or thrust generation) caused by wing flapping. Another flight pioneer, Chanute, noted in his book [5], published in 1894, that the potential of flapping-wing aircraft was held back by the limited understanding of the underlying aerodynamics. However, the success of the Wright brothers in 1903 with the fixed-wing aircraft concept soon convinced the aeronautical engineering community to regard the flapping-wing aircraft concept as unpromising for further development.

Part of the reason for the diminishing interest in flapping-wing aerodynamics can certainly be found in the complexity of the unsteady flow physics of flapping wings. While the correct flow physics of lift generation by an airfoil at steady incidence angle was already formulated by Kutta [14] and Joukowski [10] in 1902 and 1906, the phenomenon of thrust generation by a flapping airfoil was first explained only in 1909 and 1912 by Knoller [11] and Betz [1]. The first quantitative prediction of this thrust generation was achieved in 1922 by Prandtl's PhD student Birnbaum [3]. Further interest in the aerodynamics of oscillating airfoils was sparked by the need to predict the phenomenon of airfoil flutter which led to the development of inviscid incompressible flow solutions for oscillating airfoils by Theodorsen [23] and Küssner [13] in the 1930s. The availability of these solutions, in turn, motivated Theodorsen's associate Garrick [7] in 1936 to apply them to the prediction of the thrust generated by airfoil flapping. The advances in computing power achieved in the 1960s then made it possible for us to replace the Theodorsen/Küssner linearized solutions by nonlinear solutions using the panel concept. Finally, toward the

K.D. Jones (✉)
Naval Postgraduate School, Monterey, CA, USA
e-mail: jones@nps.edu, mplatzer@nps.edu

D. Floreano et al. (eds.), *Flying Insects and Robots*,
DOI 10.1007/978-3-540-89393-6_12, © Springer-Verlag Berlin Heidelberg 2009

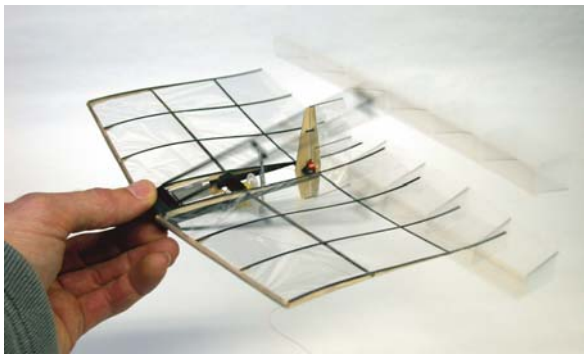

Fig. 12.1 The unusual configuration uses a trailing biplane pair of flapping wings for thrust and a large fixed wing for lift. The biplane pair takes advantage of "ground effect" without having to be near the ground, and the flow they entrain suppresses flow separation over the main wing. This third-generation radio-controlled model has a modular construction, two-channel control, a 25 cm span, 17 cm length and 13 g mass, and flies for 15 min on a single rechargeable battery

end of the century the continuing advances in computing power made it possible for us to obtain numerical solutions of the viscous flow equations.

It is fair to state that throughout the twentieth century the aeronautical engineering community showed little interest in the aerodynamics of bird and insect wings. It was only toward the end of the century that a new type of air vehicle of greatly diminished size, the micro-air vehicle (MAV), triggered a re-examination of the flapping-wing aircraft concept.

In the subsequent sections we describe our own "bio-inspired" approach that led to the development of the flapping-wing micro-air vehicle shown in Fig. 12.1. We explain the considerations which led us to a "biomorphic" flight vehicle (which does not exist in nature) instead of a "biomimetic" one (which imitates nature as closely as possible). In Sect. 12.2 we discuss the basic principles of flapping-wing aerodynamics and the experiments that pointed us toward the biplane flapping-wing arrangement. As we progressed with our research we started to realize the importance of viscous effects and the need to control flow separation. This led us to the concept of energizing a boundary layer by placing a flapping wing in the boundary layer or just downstream of a fixed wing. These analyses and experiments are described in Sects. 12.3, 12.4, 12.5. The confluence of this work, which led to the design of the MAV shown in Fig. 12.1, is described in Sect. 12.6.

12.2 Flapping Airfoil Aerodynamics

The flapping bird or insect wing presents the aerodynamicist with a complex unsteady three-dimensional flow problem because its flapping amplitude varies with the spanwise distance and its aspect ratio is often relatively small. This fact made it quite difficult for us to select a vehicle configuration which would meet our design objectives in the absence of experimental or computational aerodynamic data for flapping wings of arbitrary planform. For this reason we decided to adopt the approach historically used in the design of fixed-wing aircraft where the wing was assumed to be of sufficiently high aspect ratio so that two-dimensional airfoil data would provide a reasonable approximation of the actual three-dimensional wing aerodynamics. We felt that this assumption would yield meaningful data for birds with high aspect ratio wings, such as the albatross.

This decision was also influenced by the fact that the major analysis tools available to us were the classical linearized inviscid flow solutions for incompressible flow past oscillating airfoils developed by Theodorsen [23] and Garrick [7] and in-house panel codes for single oscillating airfoils of arbitrary profile shape written by Teng [22] and for airfoil combinations written by Pang [16]. These tools made it possible for us to analyze the effect of plunge or pitch amplitude and frequency on thrust and propulsive efficiency of single airfoils and airfoil combinations, as documented by Platzer et al. [18]. It also allowed us to study the effect of airfoil geometry and of the interference between two airfoils in close proximity to each other. Of special interest were the stationary trailing airfoil (tandem) and the opposed plunge (biplane) arrangements shown in Fig. 12.2.

Results for the tandem arrangement confirmed an earlier linearized theory result by Bosch [4] that a stationary airfoil downstream of an oscillating airfoil generates a significant amount of thrust due to the fact that the stationary airfoil converts part of the vortical energy shed by the oscillating airfoil into thrust. The results for the biplane arrangement showed that each airfoil experiences a significant thrust and propulsive efficiency increase if the airfoils are in close proximity to each other. Since this arrangement is equivalent to the flight of a single oscillating airfoil near the ground it indicated a favorable ground effect. These findings

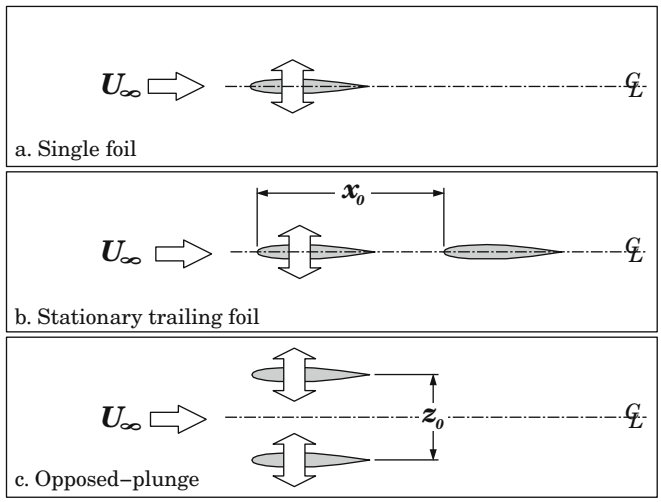

Fig. 12.2 Three configurations investigated numerically and in wind/water tunnel experiments: (a) single wing, (b) stationary trailing airfoil or tandem configuration, where the aft wing produces some thrust from the wake of the forewing, and (c) opposed plunge or biplane configuration which emulates a single wing near a ground plane

are shown in Figs. 12.3, 12.4, 12.5, and 12.6. Note that thrust (or more precisely the non-dimensional thrust coefficient) and the propulsive efficiency are plotted as a function of the non-dimensional or reduced frequency, k, and the non-dimensional amplitude of oscillation h. Here k is defined as $2\pi fc/U_\infty$, where f is the flapping frequency in H_2 and c is the chord length.

In Figs. 12.3 and 12.4 we show our computations of thrust and propulsive efficiency for the single airfoil. Note the good agreement in the prediction of

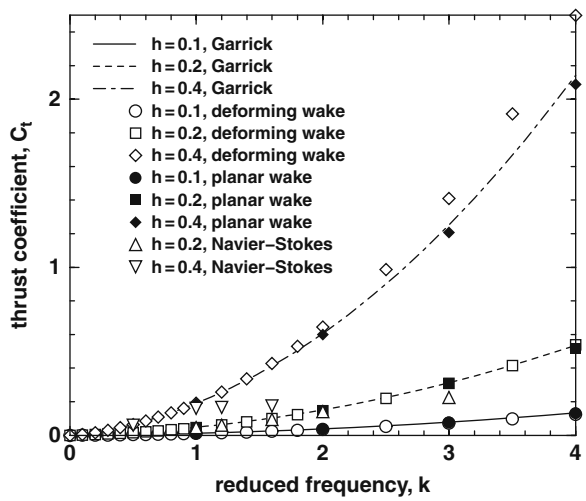

Fig. 12.3 Predicted thrust coefficient for configuration *a* as a function of plunge amplitude, h, and reduced frequency, k. The *deforming* and *planar* wake notations indicate panel solutions, where the wake evolves as it convects in the first, but the vorticity is confined to the chord line in the latter

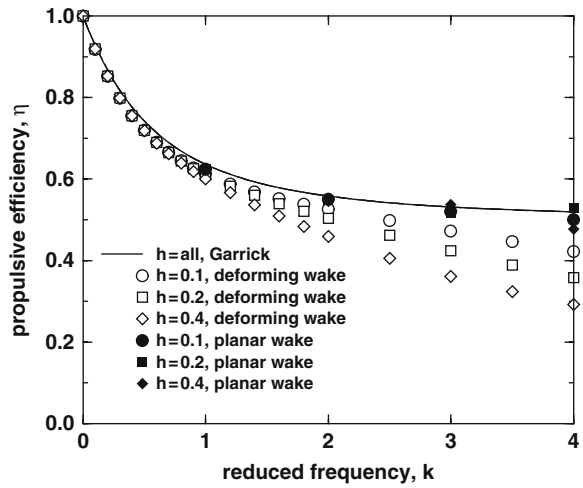

Fig. 12.4 Predicted propulsive efficiency for configuration *a* as a function of h and k

thrust between linear theory and the panel method. The Navier–Stokes predictions agree well for both h values until the product of hk gets above a critical value where leading edge separation takes over. Also note that for the panel method we have included results for both the normal wake model, where vortex elements are allowed to roll up as they convect downstream, and a wake model that forces all vorticity to remain in the plane of the chord line, as it is in linear theory. As can be seen, the deforming wake model is largely responsible for the difference between Garrick's approach and the panel code. In Figs. 12.5 and 12.6 we present a comparison between the single flapping airfoil and the tandem and biplane configurations.

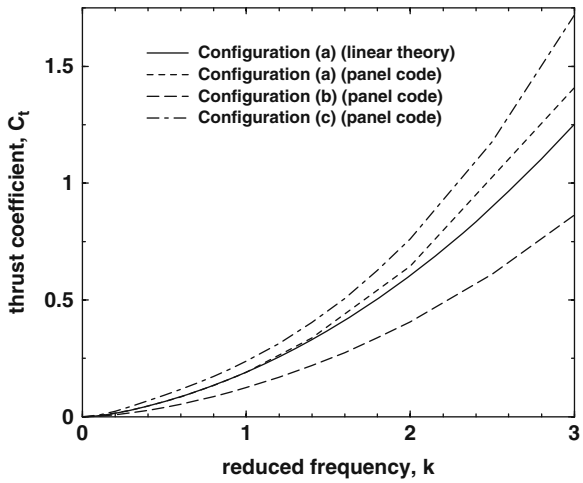

Fig. 12.5 Predicted thrust coefficient for the three configurations of Fig. 12.2. The average value for the wing pair is shown for configurations *b* and *c*. For *b* the forewing produces roughly the same thrust as the single wing and the aft wing provides some additional thrust

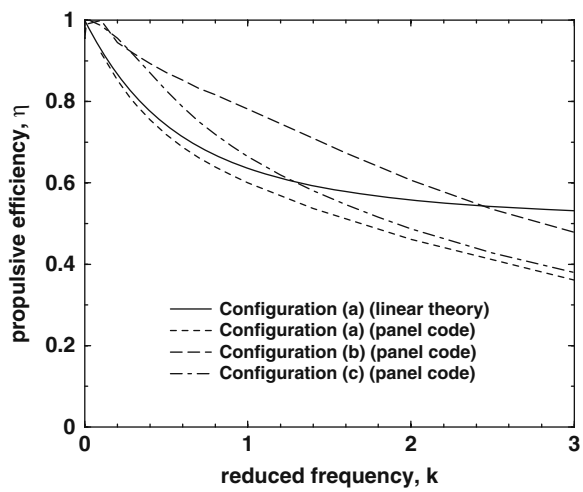

Fig. 12.6 Predicted propulsive efficiency for the three configurations in Fig. 12.2. The average value for the wing pair is shown for configurations *b* and *c*

An important unresolved question, however, was the effect of viscosity on the validity of these inviscid flow predictions. The usability of inviscid flow theory for the prediction of lift on an airfoil in a high Reynolds number flow at a small steady incidence angle is well understood because the effect of the viscous boundary layer thickness is quite small. A similar consideration also holds for the prediction of the oscillatory lift forces on an oscillating airfoil (as needed for flutter calculations). However, it is not obvious why inviscid flow theory should yield meaningful results for the force on an oscillating airfoil parallel to the flow direction (i.e., thrust), since the drag computation on a steady airfoil requires a viscous flow computation. A further important question concerns the sensitivity to Reynolds number, especially for the small Reynolds numbers encountered by micro-air vehicles.

12.3 Effect of Viscosity on Flapping Airfoil Aerodynamics

To answer these questions we conducted a series of experiments in a water channel. The panel code computations for the flow past a harmonically plunging airfoil showed the shedding of a so-called reverse Kármán vortex street from the airfoil trailing edge. As shown in Fig. 12.7, a reverse Kármán vortex street consists of counterclockwise rotating upper row vortices and clockwise rotating vortices in the lower row. This arrangement is the exact opposite of the classical Kármán vortex street shed, for example, from a stationary cylinder in a low-speed flow where the upper row vortices are turning clockwise and lower row vortices are turning counterclockwise. The change in vortex shedding from the trailing edge of a stationary airfoil to that from a harmonically plunging airfoil as the amplitude of oscillation is increased for a given frequency of oscillation is shown in Fig. 12.8. The classical Kármán vortex street shed from the stationary airfoil is shown in (a). As the airfoil starts to oscillate in plunge at a relatively low reduced frequency and amplitude, the Kármán vortex street changes into the mushroom-like vortex pattern shown in (b). As the amplitude is increased, this vortex pattern changes into the pattern shown in (c). A further increase in amplitude finally produces the reverse Kármán vortex street shown in (d). A comparison of the panel code-computed vortex street with the observed street of (d) shows excellent agreement. However, the panel code could not reproduce the vortex patterns shown in (a), (b), and (c). Hence these flow visualization experiments indicate the inadequacy of inviscid flow computations for low values of frequency, amplitude, and Reynolds number. On the other hand, they also show that there is a range of flow speed,

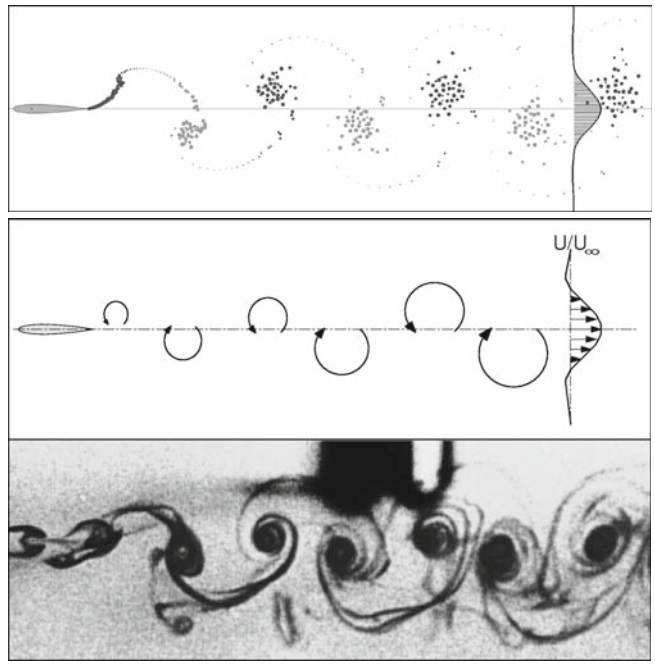

Fig. 12.7 Vortex arrangement in a thrust-indicative reverse Kármán vortex street: *top* — panel code, *middle* — schematic, *bottom* — experimental

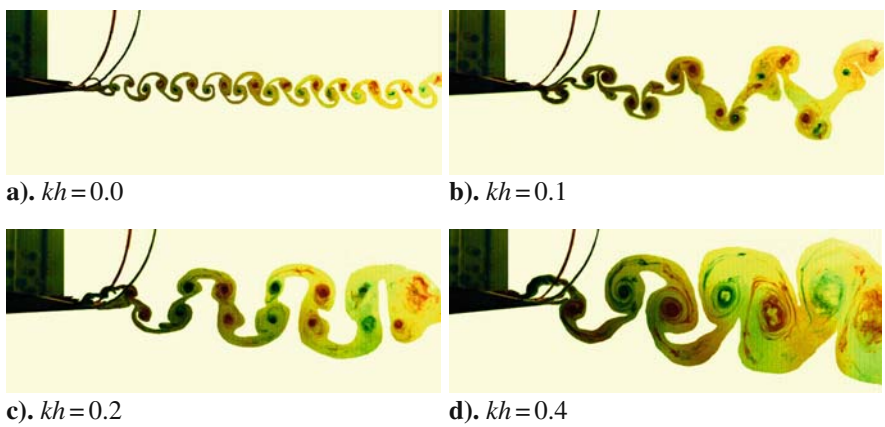

Fig. 12.8 Transition from normal to reverse Kármán vortex street with increasing *hk*. Flow is from left to right, with a heaving NACA 0012 airfoil

frequencies, and amplitudes where inviscid computations produce good agreement.

These flow visualizations were quite important. They showed that previous conclusions drawn from inviscid flow computations can be quite wrong. For example, Garrick's [7] inviscid linearized flow analysis showed that the propulsive efficiency of a harmonically plunging airfoil decreases from values close to 100% at very small reduced frequencies to only 50% for high frequencies. This led to the conclusion that very large flapping wings are required to produce meaningful thrust and efficiency values. It is now well recognized that viscous flow effects are dominant at low amplitude and frequency values and, therefore, inviscid flow analyses are highly misleading.

It is also instructive to take a closer look at the physical mechanism that causes the generation of thrust on a harmonically plunging airfoil. Consider again the reverse Kármán vortex street shown in Figs. 12.7 and 12.8d. The counterclockwise rotating vortices of the upper row and the clockwise rotating vortices of the lower row entrain flow from the outside so that a higher velocity flow is generated between the two vortex rows. Hence one would expect a jet-like flow to be

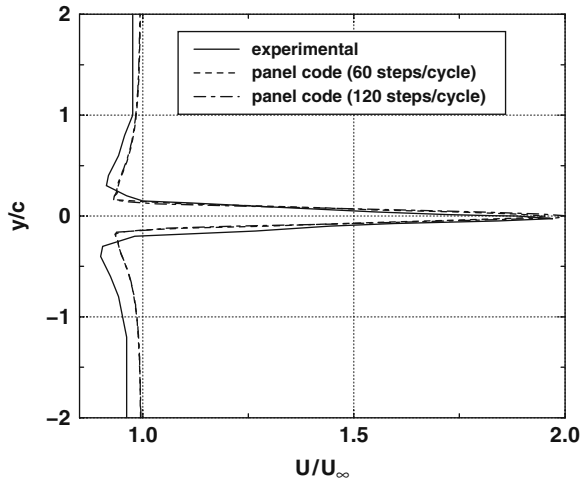

Fig. 12.9 The time-averaged jet velocity profile behind a flapping NACA 0012 measured using LDV in our water tunnel agrees well with the predictions of our inviscid panel code for moderate values of *hk*

created if one measures the time-averaged flow. This is indeed the case. In Fig. 12.9 we show one of our time-averaged flow measurements in a plane near (but downstream of) the airfoil trailing edge. It is seen that the oscillating airfoil indeed generates a distinct jet. It is also seen that the panel code-computed jet profile is in good agreement with the measurement (again proving that inviscid flow calculations can be quite adequate for certain parameter combinations). The oscillating airfoil therefore imparts momentum to the fluid in the streamwise direction which, in turn, generates a reaction force (thrust) in the opposite direction on the airfoil. The flapping bird wing therefore can be considered as a "jet engine" which came into use millions of years before the aircraft jet engine was invented and applied.

But how is the reverse Kármán vortex street generated? To answer this question, it is useful to recall the basic principle of lift generation on an airfoil. To this end it is important to remember that a so-called "starting vortex" is shed from the airfoil trailing edge whenever the airfoil's incidence angle is abruptly changed. A sudden increase in the angle of attack produces the shedding of a counterclockwise starting vortex. A decrease produces a clockwise vortex. The trailing edge has to be reasonably sharp for this shedding to occur with sufficient strength. A rounded trailing edge greatly diminishes the shedding. Consider now the airfoil as it plunges from above through the mean position. The airfoil "sees" a maximum positive angle of attack at this moment which starts to diminish greatly as it slows down. Hence the angle of attack changes from positive to negative as it reverses and reaches the maximum negative angle of attack as it approaches the mean position from below. Therefore during this part of the oscillation the airfoil will shed clockwise vorticity which accumulates quickly into the clockwise vortex of the lower row of the reverse Kármán vortex street. Similarly, while the airfoil moves above the mean position it sheds a counterclockwise vortex.

12.4 The Bird Wing — A Fully Integrated Lift/Propulsion/Control System

It has long been recognized that an aircraft's propulsive efficiency is improved when the air from the wake of the aircraft is used as part of the propulsive stream. Betz explains this in his book [2] and points out that with wake ingestion the power expended can actually be less than the product of the forward speed and craft drag. At the dawn of the jet age Smith [20] proposed to use the boundary layer air for propulsion. Similarly, Reynst [19] advocated boundary layer propulsion by means of pulsating combustors installed near the wing trailing edges. Unfortunately, the implementation of boundary layer propulsion runs into the practical difficulty of distributing the air along the wing span and ejecting it at or near the wing trailing edge. Over the years, various jet flap concepts have been developed. However, the flow losses, weight and volume penalties caused by the ducting from the jet engines to the trailing edge have always outweighed the potential benefits. Nevertheless, Leroy Smith of the General Electric Company [21] has quantified the potential benefits of wake ingestion as recently as 1993.

In contrast, birds have solved this problem in a most elegant and efficient way by means of wing flapping which, as noted above, generates a jet flow along the wing span, thus achieving a fully integrated lift/propulsion system. Furthermore, birds have mastered the use of variable camber and variable geometry concepts to adjust their wings to the required flight mode and flight control requirement.

12.5 The Oscillating Airfoil — A "Two-Dimensional" Propeller

As is clear from the preceding discussion, the oscillating airfoil can be regarded as a propeller that entrains a certain amount of flow along its span and gives it a certain amount of additional flow momentum. This fact was first fully recognized and analyzed by Birnbaum [3] who introduced the term "two-dimensional" propeller to draw attention to the fact that the oscillating airfoil works similar to the conventional propeller. This fact suggests that oscillating airfoils must have potential uses for flow entrainment and flow energization purposes.

To explore these potential uses we performed several experiments. First we considered the effect of a small oscillating airfoil mounted in the laminar boundary layer of a flat plate. The arrangement is shown in Fig. 12.10 and a typical result is given in Fig. 12.11.

It is seen that, compared to the airfoil oscillating in the outside free stream, the airfoil oscillating in the boundary layer generates a significantly increased jet flow. This suggests its use for boundary layer control by means of "blowing." In another experiment we explored the use of oscillating airfoils for flow separation control. In Fig. 12.12 flow over an airfoil with a cusped trailing edge is shown together with a small oscillating airfoil mounted close to the trailing edge. As seen in the left image, the large flow separation which occurs without flow control can be fully suppressed if the small airfoil is oscillated with a sufficiently large plunge amplitude and frequency, as seen in the right image.

12.6 Conceptual Design Considerations for a Flapping-Wing MAV

Having gathered the computational and experimental information on oscillating airfoils, described in the preceding paragraphs, we asked ourselves whether this information would suffice to design a flapping-wing micro-air vehicle. The computational and experimental results for two-dimensional flow over harmonically plunging airfoils indicated considerable potential as thrust generators (propellers). It also became clear that it might be advantageous to use high aspect ratio wings with constant spanwise oscillation amplitude. Although this choice meant a distinct deviation from the flapping wings used by birds it is clear that the diminishing amplitude of flapping bird wings near their roots contributes little to thrust production. Obviously, birds have no choice, whereas in man-made systems it is possible to take advantage of additional conceptual degrees of freedom. Furthermore, this choice reduced the need to develop computational solutions for three-dimensional flapping-wing flows and to acquire three-dimensional test results. It remained to select the most suitable oscillation mode. The two most practical oscillation modes are the plunge and pitch mode and the phase angle between these two modes (if both are selected). Rapid insight into this effect of simultaneous pitch/plunge oscillation could again be obtained with inviscid panel code computations which showed that the best propulsive efficiency is obtained if the phase angle between the pitch and plunge oscillations is 90°.

Another important conceptual design consideration concerns the number of flapping wings to be used.

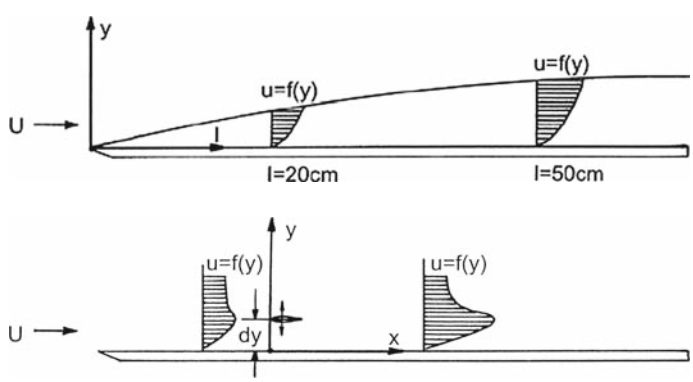

Fig. 12.10 A typical boundary layer profile is shown in the *top image*, but with the addition of a small flapping wing inside the boundary layer in the *lower image*, the boundary layer is energized, reducing drag

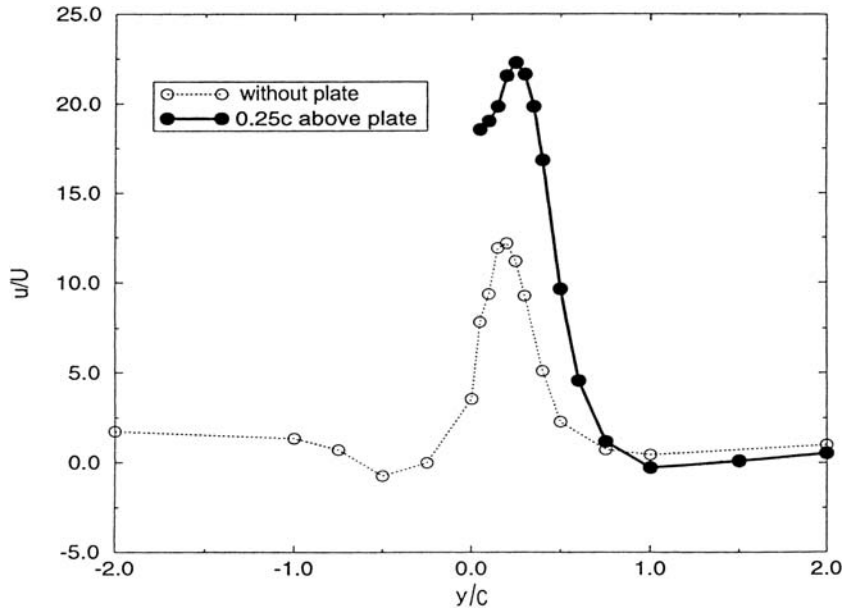

Fig. 12.11 The normalized velocity profiles measured with LDV behind a flapping wing, with the flapping wing placed in a free flow or in the boundary layer of a flat plate shows that more thrust is produced in the presence of the flat plate

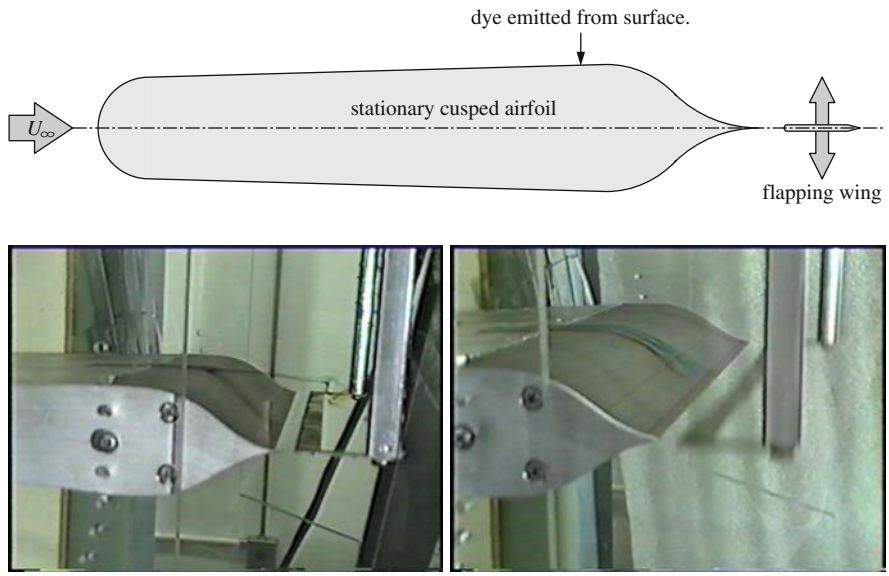

Fig. 12.12 In a water tunnel experiment, a very small flapping wing was placed in the wake of a large stationary airfoil which had a cylindrical leading edge and a cusped trailing edge. Dye was emitted from the upper surface just ahead of the cusped trailing edge. Without flapping, the flow immediately separates, and indicates a large, unsteady separated flow region. With flapping, the recirculation is greatly reduced, and the flow reattaches to the trailing edge

Birds get along with just one left and right wing. Insects, on the other hand, often have two wings as, for example, the dragonfly. The test results for the harmonically plunging airfoil in the flat-plate boundary layer showed significant benefits from operation near the wall. These results suggested to simulate "ground effect" by arranging two airfoils in biplane formation and oscillating them in counterphase. While birds

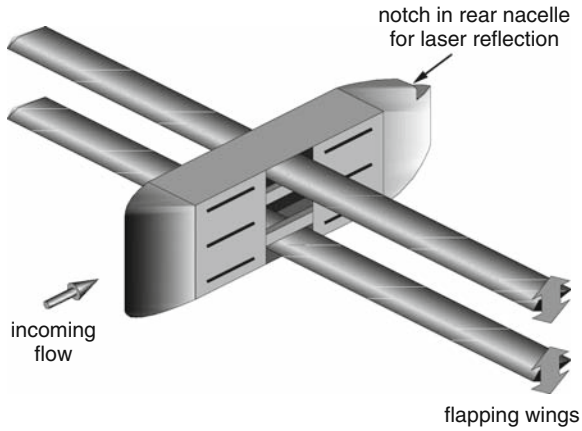

Fig. 12.13 The large biplane wind tunnel test model, with 65 mm chord, 1.2 m span wings, and a NACA 0014 airfoil section was built to investigate the performance of flapping wings in ground effect

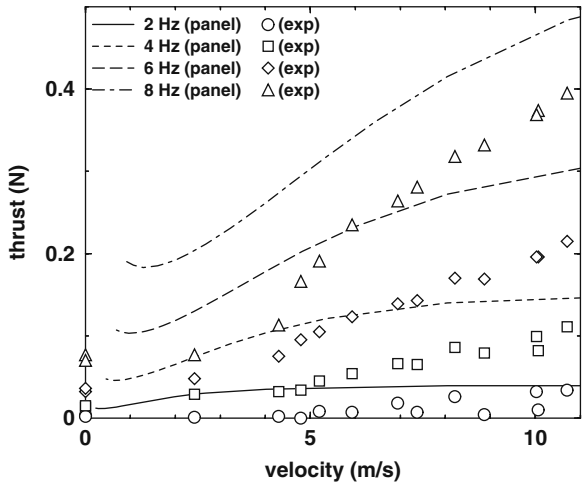

Fig. 12.15 Predicted and measured thrust for the large biplane model shown in Fig. 12.13. Reynolds numbers ranged from 0 to 50,000 and the motion was a pure plunge with amplitude $0.4c$

can only achieve this configuration by flying near the ocean's surface in true ground effect, some prehistoric insects had extensive overlap of their forewing and hindwing, according to Wootton and Kukalova-Peck [24]. The panel code computations for this case, as shown in Figs. 12.5 and 12.6, remained to be verified by direct thrust measurements. To this end, the model shown in Fig. 12.13 was built. The two wings, arranged in biplane formation, could be oscillated in either pitch or plunge. The thrust could be measured quite easily by hanging the model from the wind tunnel ceiling, as shown in Fig. 12.14, and measuring the small streamwise movement of the model with a laser range finder to estimate drag and thrust. Typical results are shown in Fig. 12.15.

These thrust measurements were quite encouraging. They then provided the motivation to build a much smaller model (of potential micro-air vehicle size) and to repeat the thrust measurements. This model is shown in Fig. 12.16 and thrust measurements are plotted in Fig. 12.17. During this phase of the micro-air vehicle development another advantage offered by the biplane

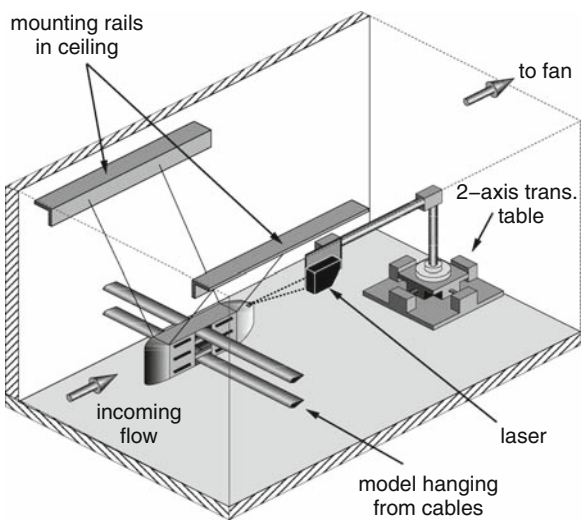

Fig. 12.14 The model was hung from the ceiling of the test section and drag/thrust was calculated by measuring the displacement of the model in the streamwise direction

Fig. 12.16 This miniaturized version of the large biplane model shown in Fig. 12.13 was built to investigate the effects of low Reynolds numbers and the use of unconventional, "insect-like" wings. The MAV-sized model had a 15 cm span, and the wings had a stiff, balsa leading edge spar and a flexible membrane surface with carbon fiber batons

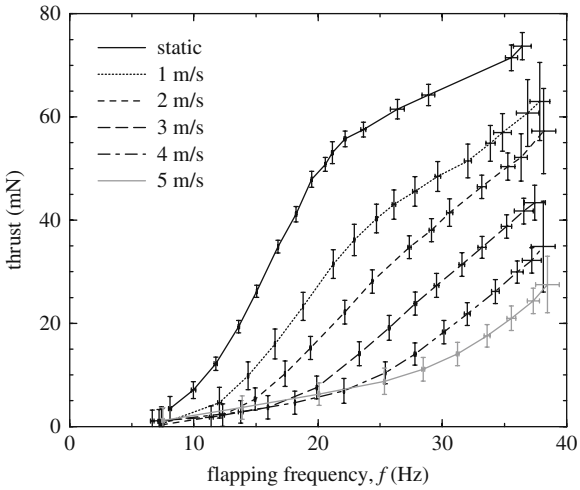

Fig. 12.17 Typical results from the 15 cm biplane test model shown in Fig. 12.16. Reynolds numbers ranged from 0 to 12,000. The drop-off at about 20 Hz is due to mechanical limitations on the elastic pitching. To achieve better performance at higher speeds, stiffer wing-mount springs were needed to limit the wing pitching

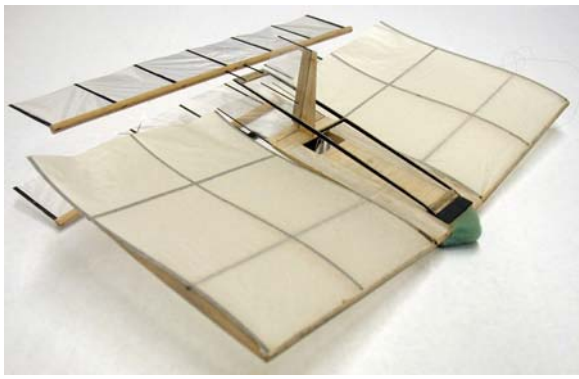

Fig. 12.18 First generation radio-controlled micro-air vehicle with throttle-only control, 30 cm span, 18 cm length, and 14.4 g mass

configuration became evident. Oscillation of two airfoils in counterphase does not affect the joint center of gravity, hence a remarkably vibration-free dynamically balanced platform is obtained if the biplane configuration is chosen. Another important advance was the excitation system which consisted of two swing arms which were driven by a crankshaft and scotch yoke combination. This mechanism oscillated the two airfoils in plunge. Yet, as discussed above, it is desirable to have a joint pitch/plunge oscillation with a 90° phasing between the two oscillations. This requirement was met by mounting the airfoils elastically at the ends of the swing arms, thus providing the airfoils with the desired pitch degree of freedom by properly adjusting the stiffness of the connection to the swing arms. Mounting this model on a rotating arm provided the final proof that adequate thrust levels could be generated by oscillating the airfoils in the 20–30 Hz frequency range.

Having thus solved the thrust-generation problem, it remained to select an aircraft configuration which would provide adequate lift and flight stability. Here again, we abstained intentionally from copying bird flight. Instead, we followed the conventional aircraft design process by separating lift and thrust generation. Selection of sufficient wing area, reflex camber for longitudinal static stability, and wing dihedral for lateral stability are well-known aeronautical design techniques. However, it remained to select the most suitable location of the flapping-wing propulsion system. This decision was greatly influenced by the flow separation control experiments of Fig. 12.18. Micro-air vehicle flight occurs in a Reynolds number range where severe flow separation problems can be expected. Arranging the flapping wings (in biplane formation) downstream but very close to the trailing edge of the stationary wing was therefore likely to minimize flow separation. Tests verified that this is indeed the case. These considerations and test results then led to the configuration of Fig. 12.18 which first flew successfully in December 2002. A short time later, refinements led to the model shown in Fig. 12.1 with modular construction, lighter materials, and much better performance.

12.7 Summary and Outlook

Since that time many versions of this micro-air vehicle have been flown countless times. The smallest version weighs approximately 6 g, with a span of 15 cm and a length of 15 cm. Using the latest Li-poly battery technology typical flight times are about 15 min. The flight speeds range between 2 and 5m/s. The maximum flight speed is limited by the achievable oscillation frequency (currently about 40 Hz). It is reasonable to expect that the flight speed can be doubled with improvements in various subsystems. The minimum speed is determined

by the stall limit. As noted before, the close-coupled wing propulsion system gives the micro-air vehicle the ability to change the angle of attack (and therefore to reduce speed) up to rather high angles of attack (typically about a 15° angle of attack for 2 m/s flight). Therefore the vehicle is amazingly gust insensitive and, after the encounter of stall, control can be regained quickly. Readers interested in more quantitative development and flight performance details can find additional information in [9, 8, and 17].

With the exception of the hummingbird, birds have only limited ability to take off vertically or to hover in the air. In fact, many large birds try to run against the wind to gain aerodynamic lift and it is sometimes amusing to observe their struggle. Our micro-air vehicle is no exception, having been inspired by birds with high aspect ratio wings. A remaining future challenge for us therefore is the development of a variation with hovering and vertical take-off and landing (VTOL) capability. Much research and development activity is presently being devoted to this challenge with some success, such as the models described in Chaps. 13 and 14, as well as the Mentor developed by SRI and the University of Toronto [12]. While our present MAV was designed with efficient cruise flight in mind, it has a distinct disadvantage for hovering flight, as the center of mass is ahead of the flapping wings. In contrast, all of the successful hovering models mentioned above have the center of mass behind the flapping wings, and should therefore obtain passive stability.

Acknowledgments We are grateful for the support received from Spiro Lekoudis of the Office of Naval Research, with project monitors Peter Majumdar and Edwin Rood, and from Richard Foch, head of the Vehicle Research Section of the Naval Research Laboratory, with project monitors Kevin Ailinger, Jill Dahlburg, and James Kellogg.

References

1. Betz, A.: Ein Beitrag zur Erklaerung des Segelfluges. Zeitschrift fuer Flugtechnik und Motorluftschiffahrt **3**, 269–270 (1912)
2. Betz, A.: Introduction to the Theory of Flow Machines. Pergamon, New York (1966)
3. Birnbaum, W.: Das Ebene Problem des Schlagenden Fluegels. Zeitschrift fuer Angewandte Mathematik und Mechanik **4**(4), 277–290 (1924)
4. Bosch, H.: Interfering airfoils in two-dimensional unsteady incompressible flow. Tech. Rep. 7, AGARD-CP-277 (1977)
5. Chanute, O.: Progress in Flying Machines. Lorenz & Herwig, Long Beach, CA (1976)
6. Dalton, S.: The Miracle of Flight. Firefly Books (1999)
7. Garrick, I.E.: Propulsion of a flapping and oscillating airfoil. Tech. Rep. 567, NACA (1936)
8. Jones, K.D., Bradshaw, C.J., Papadopoulos, J., Platzer, M.F.: Bio-inspired design of flapping-wing micro air vehicles. The Aeronautical Journal of the Royal Aeronautical Society **109**(1098), 385–392 (2005)
9. Jones, K.D., Lund, T.C., Platzer, M.F.: Fixed and Flapping Wing Aerodynamics for Micro Air Vehicle Applications, *Progress in Astronautics and Aeronautics*, vol. 195, chap. 16: Experimental and Computational Investigation of Flapping Wing Propulsion for Micro Air Vehicles, pp. 307–339. AIAA (2001)
10. Joukowski, N.: On adjoint vortices. Izviestiia **13**, 12–25 (1906)
11. Knoller, R.: Die Gesetze des Luftwiderstandes. Flug- und Motortechnik **3**(21), 1–7 (1909)
12. Kornbluh, R.D., Low, T.P., Stanford, S.E., Vinande, E., Bonwit, N., Holeman, D., DeLaurier, J.D., Loewen, D., Zdunich, P., MacMaster, M., Bilyk, D.: Flapping-wing propulsion using electroactive polymer artificial muscle actuators, phase 2: Radio controlled flapping-wing testbed. Tech. Rep. ITAD-3470-FR-03-009, SRI International (2002)
13. Kuessner, H.G.: Zusammenfassender Bericht Ueber den Instationaeren Auftrieb von Fluegeln. Luftfahrtforschung **13**(14) (1936)
14. Kutta, M.W.: Auftriebskraefte in Stroemenden Fluessigkeiten. Illustr. Aeronautische Mitteilungen (1902)
15. Lilienthal, O.: Der Vogelflug als Grundlage der Fliegekunst, 3 edn. Harenberg Kommunikation, Dortmund (1992)
16. Pang, K.C.: A computer code for unsteady incompressible flow past two airfoils. Master's thesis, Department of Aeronautics & Astronautics, Naval Postgraduate School (1988)
17. Platzer, M.F., Jones, K.D., Young, J., Lai, J.C.S.: Flapping wing aerodynamics — progress and challenges. AIAA Journal **46**(9), 2136–2149 (2008)
18. Platzer, M.F., Neace, K.S., Pang, K.C.: Aerodynamic analysis of flapping wing propulsion. AIAA-93-0484 (1993)
19. Reynst, F.H.: Pulsating Combustion. Pergamon, New York (1961)
20. Smith, A.M.O., Roberts, H.E.: The jet airplane utilizing boundary layer air for propulsion. Journal of the Aeronautical Sciences (1947)
21. Smith, L.H.: Wake ingestion propulsion benefit. Journal of Propulsion and Power **9**(1), 74–82 (1947)
22. Teng, N.H.: The development of a computer code for the numerical solution of unsteady inviscid and incompressible flow over an airfoil. Master's thesis, Department of Aeronautics & Astronautics, Naval Postgraduate School (1987)
23. Theodorsen, T.: General theory of aerodynamic instability and the mechanism of flutter. Tech. Rep. 496, NACA (1935)
24. Wootton, R.J., Kukalova-Peck, J.: Flight adaptations in palaeozoic palaeoptera. Biological Reviews of the Cambridge Philosophical Society **75**(1), 129–167 (2000)